

Prolonged PGE₂ treatment increased TTX-sensitive but not TTX-resistant sodium current in trigeminal ganglionic neurons

Xiao-Yu Zhang^a, Xi Wu^b, Peng Zhang^{a,1}, Ye-Hua Gan^{a,*}

^a Central Laboratory, Peking University School and Hospital of Stomatology, Beijing, 100081, PR China

^b Academy for Advanced Interdisciplinary Studies, College of Future Technology, Institute of Molecular Medicine, Peking University, Beijing, 100871, PR China

ARTICLE INFO

Keywords:

Electrophysiology
Inflammation
Neurophysiology
Orofacial pain/TMD
Cytokine(s)
Pharmacology

ABSTRACT

Prostaglandin E₂ (PGE₂) is an important inflammatory mediator for the initiation and maintenance of inflammatory and neuropathic pain. The acute effect of PGE₂ on sodium currents has been widely characterized in sensory neurons; however, the prolonged effect of PGE₂ remains to be determined. Here, we performed patch clamp recordings to evaluate the acute and prolonged effects of PGE₂ on sodium currents in trigeminal ganglionic (TG) neurons from male Sprague–Dawley rats. We found that 24-h treatment with PGE₂ (10 μM) increased the peak sodium current density by approximately 31% in a voltage-dependent manner and shifted the activation curve in a hyperpolarized direction but did not affect steady-state inactivation. Furthermore, treatment with PGE₂ for 24 h increased the current density of tetrodotoxin-sensitive (TTX-S) but not TTX-resistant (TTX-R) channels significantly. Interestingly, TTX-S current was increased mostly in medium-sized, but not in small-sized, neurons after 24 h of treatment with PGE₂. Moreover, the mRNA level of TTX-S Nav1.1 but not TTX-R Nav1.8 or Nav1.9 was significantly increased after 24 h of treatment with PGE₂. In contrast, 5-min treatment with PGE₂ (10 μM) increased the peak sodium current density by approximately 29% and increased TTX-R sodium currents, but not TTX-S currents, in both small- and medium-sized TG neurons. Our results presented a differential regulation of subtypes of sodium channels by acute and prolonged treatments of PGE₂, which may help to better understand the mechanism of PGE₂-mediated orofacial pain development.

1. Introduction

Prostaglandin E₂ (PGE₂) is an important inflammatory mediator that induces the onset and maintenance of inflammatory and neuropathic pain (Petho and Reeh, 2012). PGE₂ at the injury site is increased simultaneously with the onset of postoperative pain after dental or hip surgery in patients (Buvanendran et al., 2006; Dionne et al., 2003; Roszkowski et al., 1997). In the carrageenan-induced inflammatory pain model, the increase in PGE₂ lasted for several days at the inflammatory site of the paw or knee (Dirig and Yaksh, 1999; Guay et al., 2004). In the spinal nerve ligation (SNL)-induced neuropathic pain model, the increase in PGE₂ lasts from months to years at the site of nerve injury (Ma et al., 2010; Ma and Eisenach, 2003; Treutlein et al., 2018). Cyclooxygenases (COXs), the key enzymes for PGE₂ synthesis, are targets for many nonsteroidal anti-inflammatory drugs for attenuating human and animal inflammatory pain symptoms (Liu et al., 2020; Ma et al., 2010;

Samad et al., 2002). In our previous study, we found that PGE₂ facilitates temporomandibular joint (TMJ) inflammatory pain by increasing the mRNA and protein levels of the voltage-gated sodium channel Nav1.7 in the trigeminal ganglion (TG) (Zhang et al., 2018a; Zhang and Gan, 2017). However, the details of how functional sodium currents are modulated by PGE₂ in TG neurons remain unknown.

Voltage-gated sodium (Nav) currents are key players in generating neuronal activity during pain transduction (Dib-Hajj et al., 2010). According to their sensitivity to tetrodotoxin (TTX), sodium channels are classified into TTX-sensitive (TTX-S) and TTX-resistant (TTX-R) subtypes (Bennett et al., 2019). TTX-S channels, including Nav1.1, Nav1.3, Nav1.6, Nav1.7, and TTX-R channels, including Nav1.8 and Nav1.9, are all expressed in adult peripheral sensory neurons (Bennett et al., 2019; Dib-Hajj et al., 2010). TTX-R channels are mainly expressed in small- and medium-sized dorsal root ganglion (DRG) or TG neurons (Djouhri and Lawson, 2004; Nakamura et al., 2016). Acute exposure to PGE₂ for

* Corresponding author. Central Laboratory, Peking University School and Hospital of Stomatology, 22 Zhongguancun South Street, Haidian District, Beijing, 100081, China.

E-mail address: kqyehuagan@bjmu.edu.cn (Y.-H. Gan).

¹ Current address: Department of Oral and Maxillofacial Surgery, Qingdao Municipal Hospital, Shandong Province, Qingdao 266011, P.R. China.

several minutes increases the TTX-R current by approximately 30% in small TG neurons (Kadoi et al., 2007; Liu and Duan, 2016), while how PGE₂ affects TTX-S current in TG neurons has not yet been determined. In DRG neurons, several minutes of exposure to PGE₂ increases the TTX-R current in approximately 50% of small-to medium-sized neurons but has no effect on the TTX-S component in PGE₂-responsive DRG neurons (England et al., 1996; Gold et al., 1996, 1998; Vaughn and Gold, 2010). Although DRG and TG share many functional and molecular similarities (Lopes et al., 2017; Megat et al., 2019), there is still a lack of evidence on whether PGE₂ affects subtypes of sodium currents in DRG and TG in the same way.

Subtypes of sodium channels in DRG sensory neurons have been found to be differentially modulated in persistent pain models (Basbaum et al., 2009). The currents of TTX-S and TTX-R were increased in parallel in small afferent DRG neurons after carrageenan injection in the hind paw (Black et al., 2004b; Tanaka et al., 1998; Tate et al., 1998). However, in a chronic constriction injury-induced neuropathic pain model, only the TTX-S current is increased, while the TTX-R sodium current is reduced in small DRG neurons (Dib-Hajj et al., 1999; Kral et al., 1999). The acute effect of PGE₂ on sodium currents in DRG and TG neurons involves cAMP/PKA-dependent phosphorylation of the sodium channel (England et al., 1996; Fitzgerald et al., 1999; Gold et al., 1998; Liu and Duan, 2016; Tripathi et al., 2011). However, prolonged exposure of PGE₂ to DRG from 12 h to 5 days fails to activate PKA due to its desensitization (Malty et al., 2016), raising the question of whether PGE₂ affects sodium channels differently between acute and prolonged treatments.

In this study, we performed patch clamp electrophysiology in TG neurons and investigated the effects of acute and 24-h PGE₂ treatments on TTX-S and TTX-R sodium currents in small-to medium-sized neurons with both TTX-S and TTX-R currents. The results showed that both acute and prolonged PGE₂ treatments increased sodium currents in a voltage-dependent manner in small-to medium-sized neurons. Treatment with PGE₂ for 24 h increased the TTX-S but not the TTX-R current density, and the increase in TTX-S occurred mainly in medium-sized but not in small-sized TG neurons. In comparison, acute PGE₂ exposure increased current through TTX-R, but not TTX-S, in small- and medium-sized TG neurons. These results may help uncover the different functions of TTX-S and TTX-R in PGE₂-mediated orofacial persistent pain development.

2. Material and methods

2.1. Cell preparation

All experiments were performed according to the protocol approved by the Animal Use and Care Committee of Peking University in China. Freshly isolated TG neurons were prepared from specific pathogen-free 100–120 g male Sprague Dawley rats after decapitation as previously described (Liu et al., 2021). TGs were collected in L15 medium at 4 °C and were cut into pieces to be digested later with collagenase IA (Sigma Chemicals, St. Louis, MO, USA; 1 mg/mL) and trypsin I (Sigma Chemicals, St. Louis, MO, USA; 0.3 mg/mL) at 37 °C for 40 min. Individual cells were dissociated by triturating through pipettes and then plated onto poly-L-lysine pretreated dishes containing F12 medium (Invitrogen, Carlsbad, CA, USA) for incubation (Supplemental Table 1). Small- (<30 pF) to medium-sized (30–70 pF) TG neurons were used 1–8 h after preparation as freshly isolated neurons to study the acute effect of PGE₂ (10 μM) or vehicle (0.1% ethanol). PGE₂ has a short half-life, equal to approximately 30 h in standard culture medium at 37 °C (Watzet et al., 2009); thus, the prolonged effect of PGE₂ was examined by incubation in medium with PGE₂ (10 μM) or vehicle for 24–30 h.

2.2. Patch-clamp recording

Whole-cell recording was performed using an EPC/10 amplifier (HEKA Elektronik, Lambrecht, Pfalz, Germany) and PatchMaster

Software on small- or medium-sized TG neurons with a cellular capacitance between 15 and 70 pF. Patch pipettes with 1–2 MΩ resistance were used during voltage clamp procedures. Capacitance transients and series resistance were compensated, and 85%–95% series resistances compensation were used to minimize voltage errors. The liquid junction potential was not adjusted. A P/4 protocol was used to subtract the leak current. The cells with series resistances larger than 20 MΩ or with a difference of more than 20% were excluded. For the sodium current recording, the extracellular solution contained (in mM): 60 NaCl, 3 KCl, 2.5 CaCl₂, 3 MgCl₂, 10 HEPES, 0.1 CdCl₂, 10 tetraethylammonium chloride (TEA-Cl), and 10 glucose, 110 sucrose (pH 7.4 adjusted with NaOH). TEA-Cl and CdCl₂ were puffed extracellularly onto the neurons to block endogenous voltage-gated potassium and calcium channels. The intracellular solution contained (in mM): 145 CsCl, 5 NaCl, 1 CaCl₂, 2 MgCl₂, 2 Mg2ATP, 10 HEPES, 10 EGTA, and 1 NaGTP (pH 7.2 with CsOH). PGE₂ was stocked as 10 mM in ethanol and diluted to 10 μM with extracellular solution or culture medium for the acute or prolonged effect, respectively. TTX was stocked as 1 mM in ddH₂O and diluted to 1 μM with extracellular solution. Vehicle (0.1% ethanol) was used for the control group. All drugs were from Sigma.

2.3. Voltage protocols

Neurons were depolarized from a holding potential of –100 mV to a series of voltage steps from –80 to 20 mV (at 5 mV steps) for 50 ms at an interval of 1 s to obtain current-voltage (*I*–*V*) relationships and activation curves as previously described (Zhang et al., 2018b). The sodium conductance (*G*) was calculated from $G = I / (V - V_{rev})$, where *I* is the peak current during voltage steps (*V*), and *V*_{rev} is the reversal potential of the sodium channel. For steady-state inactivation curves, cells were held at conditioning potentials from –120 mV to 0 mV (at 5 mV steps) for 200 ms and then depolarized to a –10 mV test pulse for 50 ms at an interval of 1 s. A Boltzmann function was used to fit the activation and inactivation curves: G/G_{max} (or I/I_{max}) = $[1 + \exp((V_m - V_{half})/k)]^{-1}$, where *V*_{half} is the half-activated voltage, *k* is the slope factor, and *V*_m is the membrane potential. The current density of the sodium current was calculated by dividing the peak value by the membrane capacitance.

For the separation of TTX-S or TTX-R currents, cells were depolarized from –120 mV (200 ms duration) to –10 mV for 50 ms to record the total sodium current, and TTX-R current was elicited in two ways: from a preinactivation voltage of –50 mV (200 ms duration) to –10 mV for 50 ms (without TTX) or from –120 mV (200 ms duration) to –10 mV for 50 ms in the presence of TTX (0.5 μM). Then, the TTX-S current was calculated by subtracting the TTX-R current from the total sodium current digitally.

2.4. Statistics

Data were analysed with Igor software (Wavemetrics, Lake Oswego, Oregon) and GraphPad Prism (GraphPad Software, San Diego, CA) and are shown as the mean ± SEM. Significance changes were tested using one-way ANOVA, two-tailed unpaired or paired Student's *t*-test, and the Mann–Whitney test as indicated (**P* < 0.05).

3. Results

3.1. PGE₂ increased sodium currents at 24 h posttreatment in small-to medium-sized TG neurons

We first examined the effect of PGE₂ (10 μM) on sodium current at 24 h posttreatment. Sodium currents were elicited by a series of voltage steps for 50 ms from a holding potential of –100 mV, and we observed that PGE₂ (10 μM) increased the peak value of sodium current density by 31% compared with the vehicle group at 24 h posttreatment in small-to medium-sized TG neurons (Fig. 1, A–C; control: *n* = 32 neurons from 12 rats; PGE₂: *n* = 35 neurons from 12 rats; unpaired Student's *t*-test, *t*

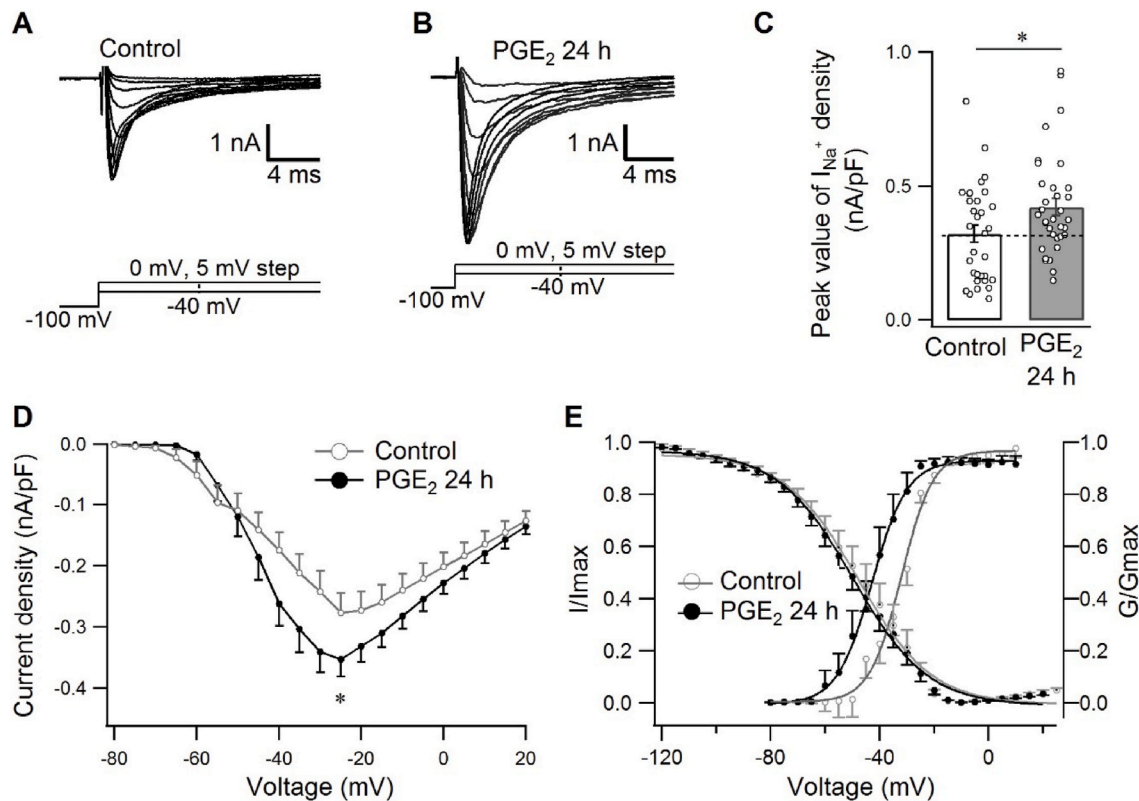


Fig. 1. Effect of PGE₂ on sodium currents at 24 h posttreatment in small-to medium-sized TG neurons. **(A, B)** Representative traces showing depolarization-induced sodium current density at 24 h posttreatment with vehicle (control, **A**) or PGE₂ (10 μ M, **B**). Cells were depolarized from -40 mV to 0 mV for 50 ms from a holding potential of -100 mV. **(C)** Statistics showing the effect of PGE₂ on the peak value of the total sodium current density at 24 h posttreatment. Cells were depolarized to a range of potentials from -80 mV to 20 mV for 50 ms from a holding potential of -100 mV. Currents were normalized to the membrane capacitance. **(D)** I–V curves of sodium current obtained at 24 h posttreatment with vehicle (control) or PGE₂ in TG neurons. Currents were normalized to the membrane capacitance. **(E)** Comparison of the activation and steady-state inactivation curves between the control and PGE₂ groups. Conductances and currents were normalized to the peak value during the activation and inactivation pulses. Error bar, SEM. * $P < 0.05$, unpaired Student's *t*-test for **(C)**, **(D)** and **(E)**.

(2.212) = 65, $P = 0.0305$). The membrane capacitances of the control group and PGE₂ group were 29.36 ± 2.25 pF and 24.59 ± 1.49 pF, respectively (control: $n = 32$ neurons from 12 rats; PGE₂: $n = 35$ neurons from 12 rats; Mann–Whitney test, $U = 479$, $P = 0.3129$). Furthermore, the I–V curve showed that PGE₂ (10 μ M) increased the current density, especially at -25 mV, compared to the control (Fig. 1D, $n = 35$ neurons from 12 to 13 rats for each group, unpaired Student's *t*-test, $t(2.049) = 68$, $P = 0.0443$). Then, we studied the 24 h effect of PGE₂ (10 μ M) on the voltage-gating properties of sodium currents, including activation and inactivation of sodium currents, and observed that PGE₂ (10 μ M) did not affect the voltage dependence of steady-state inactivation (control: $n = 13$ neurons from 9 rats; PGE₂: $n = 24$ neurons from 9 rats; $V_{\text{half}} = -45.00 \pm 3.75$ for control and $V_{\text{half}} = -47.18 \pm 0.64$ for the PGE₂ group, unpaired Student's *t*-test, $t(0.4574) = 35$, $P = 0.6502$) but shifted the activation curve to the hyperpolarizing direction (control: $n = 19$ neurons from 10 rats; PGE₂: $n = 18$ neurons from 11 rats; $V_{\text{half}} = -32.71 \pm 2.03$ mV for control and $V_{\text{half}} = -41.55 \pm 2.59$ mV for the PGE₂ group, unpaired Student's *t*-test, $t(2.691) = 35$, $P = 0.0108$) (Fig. 1E), lowering the threshold for the activation of sodium current in small-to medium-sized TG neurons.

3.2. PGE₂ increased TTX-S but not TTX-R currents at 24 h posttreatment in small-to medium-sized TG neurons

We separated the TTX-R from the total current in cultured TG neurons in two ways: from a preinactivation voltage of -50 mV (200 ms) to -10 mV for 50 ms (TTX-R₁) or by depolarizing neurons from -120 mV to -10 mV with TTX (0.5 μ M) in the extracellular solution (TTX-R₂) (Fig. 2A) (Black et al., 2004a; Cummins and Waxman, 1997). The peak

values of current density for TTX-R₁ and TTX-R₂ were comparable (Fig. 2B, $n = 21$ neurons from 7 rats for each group, one-way ANOVA, $F(2, 40) = 55.21$, $P = 0.5929$), confirming that the two protocols were equally applicable. Because the preinactivation method was faster and easier, we used it to examine the effect of PGE₂ (10 μ M) on the TTX-R current. Most of the TG neurons ($74/79$ neurons) exhibited both TTX-S and TTX-R currents, and only a minority ($5/79$) exhibited only TTX-S currents. We studied the effect of 24-h PGE₂ (10 μ M) treatment on TTX-R currents in TG neurons that contained both TTX-R and TTX-S channels and observed that prolonged PGE₂ treatment did not significantly affect the current density of TTX-R (Fig. 2C and D; control: $n = 32$ neurons from 12 rats; PGE₂: $n = 35$ neurons from 12 rats; Mann–Whitney test, $U = 551.5$, $P = 0.9181$).

Furthermore, TTX-S (TTX-S₁ or TTX-S₂) currents were calculated by digitally subtracting the TTX-R₁ or TTX-R₂ currents, respectively, from the total sodium currents when neurons were depolarized to -10 mV for 50 ms (Fig. 3A). The amplitudes of TTX-S₁ and TTX-S₂ were comparable (Fig. 3A, $n = 21$ neurons from 7 rats for each group; unpaired Student's *t*-test, $t(0.7428) = 40$, $P = 0.4619$). Because the preinactivation method was faster and easier, we used it to examine the effect of PGE₂ on the TTX-S current. Then, we compared the effect of PGE₂ (10 μ M) on TTX-S after 24 h of treatment and observed that the TTX-S current density was increased by approximately 57% in the PGE₂ group compared to that of the control (Fig. 3B and C; control: $n = 32$ neurons from 12 rats; PGE₂: $n = 35$ neurons from 12 rats; Mann–Whitney test, $U = 358$, $P = 0.0107$). As TTX-S channels can be activated by a low activation threshold (Bennett et al., 2019), its increase may explain the hyperpolarizing shift of the activation curve of the total sodium current after 24 h of treatment with PGE₂.

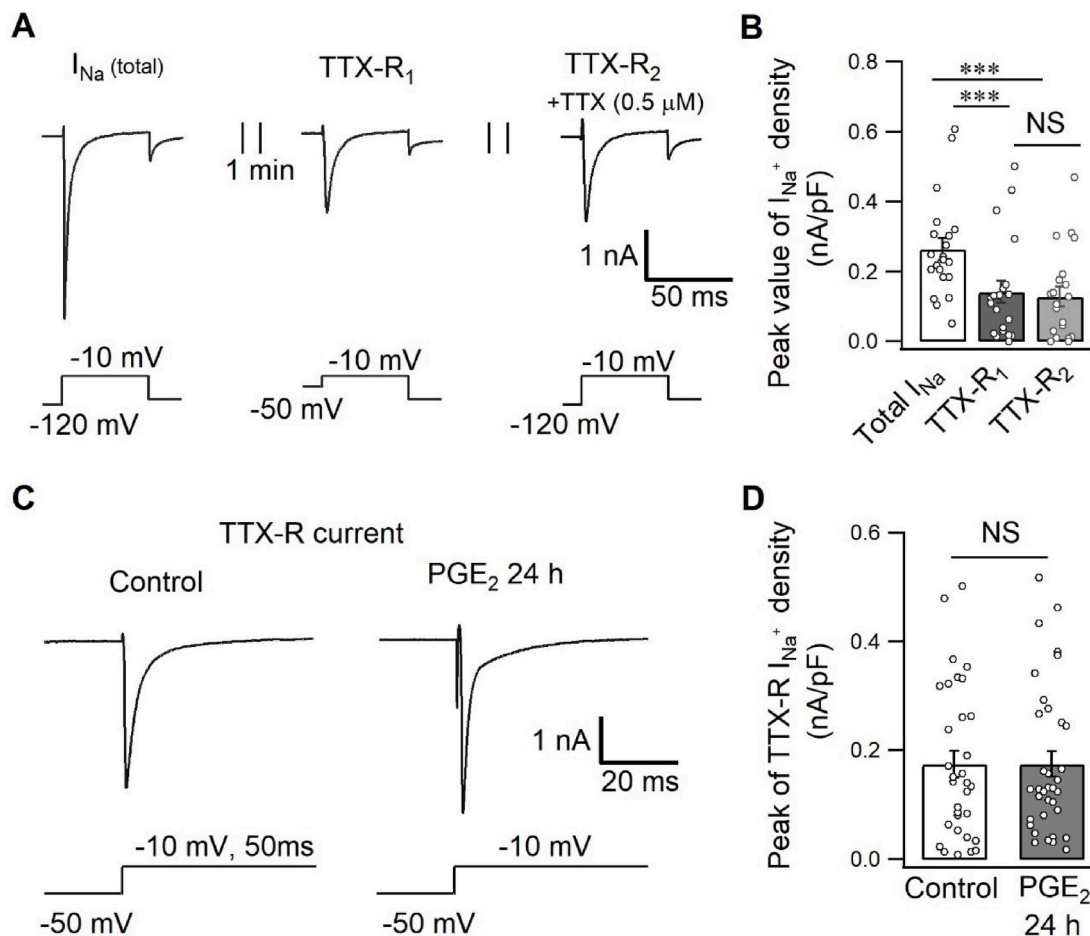


Fig. 2. Intact TTX-R current in TG neurons at 24 h posttreatment with PGE₂. (A) TTX-R was elicited in two ways: from a preinactivation voltage of -50 mV for 200 ms to a test pulse of -10 mV for 50 ms (TTX-R₁) or from a conditioning voltage of -120 mV for 200 ms to the test pulse of -10 mV for 50 ms in the presence of TTX (0.5μ M) (TTX-R₂), and the total sodium peak current was excited from -120 mV (200 ms duration) to a test pulse of -10 mV for 50 ms. (B) Statistics showing the current density of TTX-R₁ was comparable to that of TTX-R₂. (C) Representative trace showing the TTX-R current at 24 h posttreatment with vehicle (control) or PGE₂ (10μ M). (D) Statistics showing no significant effect of PGE₂ on TTX-R peak current density. Error bar, SEM. NS, no significance. *** $P < 0.001$, one-way ANOVA for B, Mann-Whitney test for D.

3.3. PGE₂ treatment increased TTX-S current mainly in medium-sized TG neurons at 24 h posttreatment

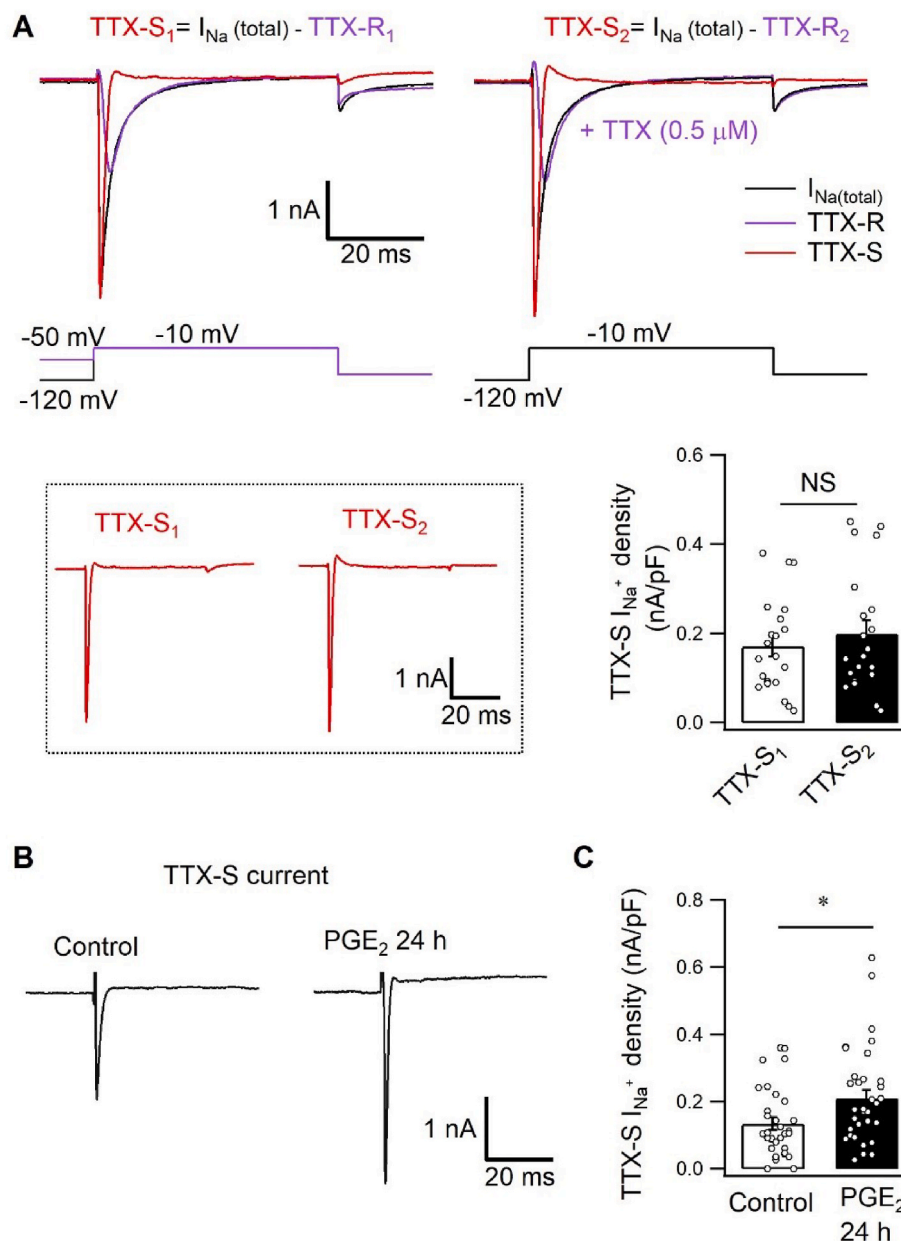
To further determine whether PGE₂ differentially affected TTX-R and TTX-S currents in different-sized neurons, TTX-R and TTX-S currents from the small- ($C_m < 30$ pF) and medium-sized (30 pF $< C_m < 70$ pF) TG neurons were quantified at 24 h post-treatment with PGE₂ (10μ M). We observed that the TTX-R current was not significantly affected by PGE₂ (10μ M) in either small- or medium-sized neurons (Fig. 4A and B, small: $n = 21$ neurons and 28 neurons from 11 to 13 rats for the control and PGE₂ groups; unpaired Student's t -test, $t(0.8270) = 47$, $P = 0.4124$; medium: $n = 11$ neurons and 7 neurons from 6 to 7 rats for the control and PGE₂ groups; unpaired Student's t -test, $t(1.104) = 16$, $P = 0.2859$). The TTX-R current density at each individual neurons was plotted against membrane capacitance, showing that relative higher levels of TTX-R currents were preferentially clustered in the small neurons other than medium-sized neurons (Fig. 4B). Interestingly, The TTX-S current density at each individual neurons and the averaged TTX-S current density showed potentiated effect by 24-h treatment with PGE₂ (10μ M) in medium-sized neurons but not in small-sized neurons (Fig. 4C and D, small TG neurons: $n = 19$ neurons and 25 neurons from 11 to 13 rats or the control and PGE₂ groups; medium TG neurons: $n = 11$ neurons and 7 neurons from 6 to 7 rats for the control and PGE₂ groups; small TG neurons: unpaired Student's t -test, $t(1.493) = 47$, $P = 0.1421$; medium TG neurons: unpaired Student's t -test, $t(3.005) = 16$, $P = 0.00849$).

3.4. PGE₂ treatment increased TTX-S Nav1.1 mRNA in TG explants at 24 h posttreatment

In our previous work, we have found that 24 h-exposure of PGE₂ increased mRNA and protein levels of TTX-S channel Nav1.7. Beside this, we performed real-time PCR experiment to test effect of PGE₂ on mRNA levels of the other channels, and observed that 24-h-treatment of PGE₂ also increased the TTX-S channels Nav1.1 significantly (Supplemental Fig. 1, $n = 8$ TG explants from 8 rats, $P = 0.0273$, Wilcoxon matched-pairs signed rank test), and had no significant effect on the mRNA levels of TTX-R channels Nav1.8 and Nav1.9, and TTX-S channels Nav1.3 and Nav1.6 (Supplemental Fig. 1, $n = 8$ TG explants from 8 rats for each group, $P = 0.3125$ for Nav1.3; $P = 0.6875$ for Nav1.6; Wilcoxon matched-pairs signed rank test for Nav1.3 and Nav1.6; $P = 0.2482$ for Nav1.8, $t(1.260) = 14$ for Nav1.8; $P = 0.4370$ for Nav1.9, $t(0.8243) = 14$ for Nav1.9; Paired Student's t -test for Nav1.8 and Nav1.9). This result is consistent with our present data showing that 24-h exposure of PGE₂ increased TTX-S current but not TTX-R current, which suggests that both Nav1.7 and Nav1.1 may contribute to the upregulation of TTX-S current.

3.5. Acute PGE₂ treatment increased TTX-R but not TTX-S currents in small-to medium-sized TG neurons

To compare with the prolonged effect of PGE₂, we determined the acute effect of PGE₂ on subtypes of sodium channels in small-to medium-



sized TG neurons. We examined sodium currents after the application of PGE₂ or vehicle for 5 min on freshly isolated small-to medium-sized TG neurons following a series of potentials for 50 ms in TG neurons. We observed that the peak values of sodium currents were increased by approximately 29% evoked by voltage steps from -80 mV to 20 mV from a holding potential of -80 mV at 5 min post-PGE₂ (10 μM) application compared with the vehicle-treated group (Fig. 5A and B, *n* = 11 neurons from 5 rats for vehicle and *n* = 36 neurons from 11 rats for PGE₂ group, Mann-Whitney test, *U* = 115, *P* = 0.0396), and 50% (18/36) of the examined neurons were PGE₂-responsive neurons. The I-V curve showed that sodium current density was increased by PGE₂ (10 μM) in a voltage-dependent manner, especially between -10 mV and 0 mV in PGE₂-responsive neurons (Fig. 5C, *n* = 10 neurons from 7 rats, -10 mV: paired Student's *t*-test, *t*(3.138) = 6, *P* = 0.0201; -5 mV: paired Student's *t*-test, *t*(3.005) = 6, *P* = 0.0239; 0 mV: paired Student's *t*-test, *t*(2.652) = 6, *P* = 0.0379; Paired Student's *t*-test was performed between the same voltage-steps before and after PGE₂ application).

Next, we examined the effect of PGE₂ in small- and medium-sized freshly-isolated TG neurons separately and observed that TTX-R

current density was increased by 5-min PGE₂ (10 μM) treatment by approximately 28% and 38% in small- and medium-sized TG neurons, respectively (Fig. 5D and E, small TG neurons: *n* = 6 neurons from 5 rats, paired Student's *t*-test, *t*(4.207) = 5, *P* = 0.0084; medium TG neurons: *n* = 5 neurons from 3 rats, paired Student's *t*-test, *t*(5.714) = 4, *P* = 0.0046), while TTX-S current density was not significantly affected either in small- or medium-sized TG neurons (Fig. 5D and E, *P* > 0.05, small TG neurons: *n* = 6 neurons from 5 rats, paired Student's *t*-test, *t*(1.127) = 5, *P* = 0.3110; medium TG neurons: *n* = 5 neurons from 3 rats, paired Student's *t*-test, *t*(0.9168) = 4, *P* = 0.4111). We also studied the acute effect of PGE₂ on 24-h cultured neurons after vehicle application, and observed that acute treatment of PGE₂ (10 μM) increased the peak value of sodium current density, and TTX-R but not TTX-S current was significantly increased in 24 h-cultured small-to-medium sized TG neurons (data not shown).

4. Discussion

Here, we demonstrated a differential modulatory effect of PGE₂ on

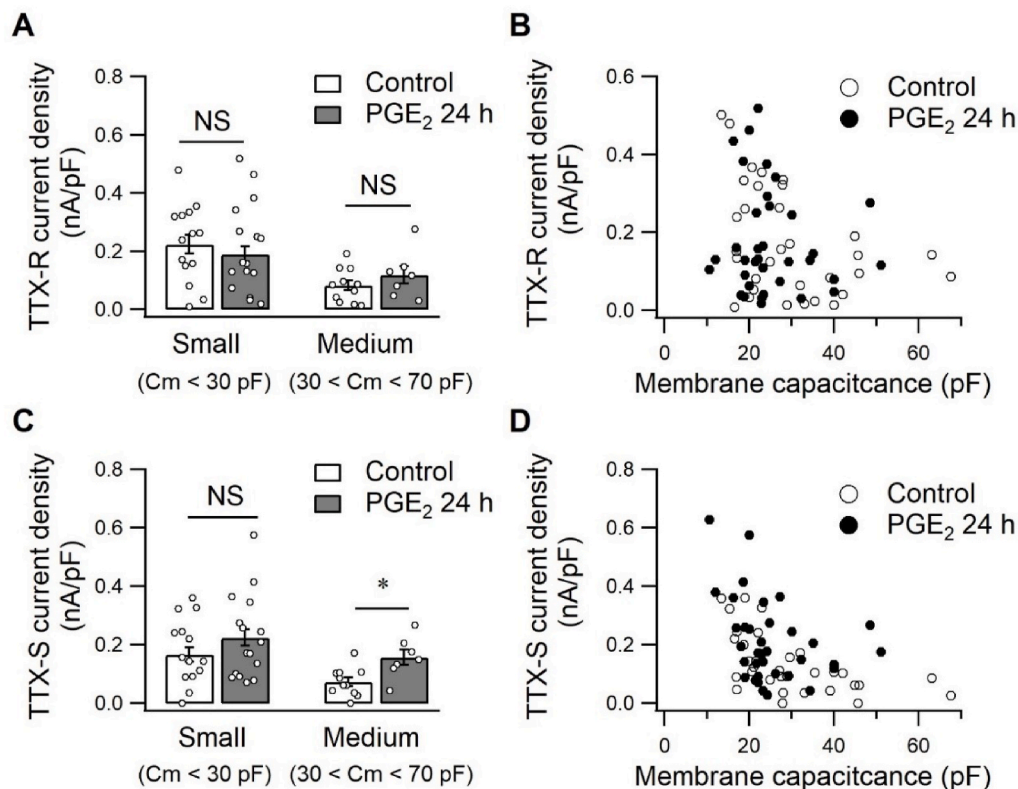


Fig. 4. Effect of PGE₂ on TTX-R and TTX-S current density in small- and medium-sized neurons in the total sodium current at 24 h posttreatment. (A) TTX-R current density obtained in either small- or medium-sized TG neurons at 24 h posttreatment with vehicle (control) or PGE₂ (10 μM). (B) TTX-R current density versus membrane capacitance in the vehicle (control) and PGE₂ (10 μM) groups. (C) TTX-S current density obtained in either small- or medium-sized TG neurons after 24 h of treatment with vehicle (control) or PGE₂ (10 μM). (D) TTX-S current density versus membrane capacitance in the vehicle (control) and PGE₂ groups (10 μM). NS, no significance. Error bar, SEM. **P* < 0.05, unpaired Student's *t*-test for (A) and (B).

subtypes of sodium channels in TG neurons after acute and prolonged treatments. 5-min and 24-h PGE₂ (10 μM) treatment increased sodium currents in small- to medium-sized TG neurons, while their modulation on TTX-S and TTX-R subtypes were different: 5-min treatment of PGE₂ increased TTX-R but not TTX-S current both in small and medium-sized TG neurons, while 24-h treatment of PGE₂ increased TTX-S but not TTX-R current mainly in medium- but not small-sized TG neurons.

TG neurons were classified as small sized TG neurons (<30 μm, 23.5 ± 5.9 pF) which exhibited both TTX-S and TTX-R current, and large sized TG neurons (>40 μm, 106.1 ± 18.5 pF) which exhibited only TTX-S sodium current (Nakamura et al., 2016; Xu et al., 2010), so for this reason we classified TG neurons as small (<30 pF) and medium (30–70 pF). Acute treatment with PGE₂ (10 μM) increased TTX-R but not TTX-S currents in 50% of small- to medium-sized TG neurons. Previous studies have reported that acute PGE₂ treatment increased TTX-R Nav1.8 and Nav1.9 in a population of small- to medium-sized TG neurons (Kadoi et al., 2007; Liu and Duan, 2016). We confirmed the results in our study and further observed that there was little effect on the TTX-S current after acute PGE₂ treatment in TG neurons, which is similar to previous results in the DRG (Gold et al., 1996; Vaughn and Gold, 2010). The percentage of PGE₂-responsive TG neurons in our study is also consistent with previous DRG results (England et al., 1996; Gold et al., 1996, 1998). The increase in TTX-R by acute PGE₂ treatment could contribute to the neuronal activity by increasing the frequency and lowering the threshold of action potentials in dorsal root ganglion neurons within several minutes (Davidson et al., 2016; Gold and Traub, 2004) and also in trigeminal ganglion sensory neuron (Kadoi et al., 2007; Liu and Duan, 2016). TTX-R Nav1.9 has an inactivation voltage of -40 mV, which is lower than that of Nav1.8 (Cummins et al., 1999), and, because we recorded the TTX-R current at an inactivation voltage of -50 mV, the two isoforms were not discriminable by the protocol. However, as the Nav1.9 current is more prominent in fluoride-based intracellular solutions than in chloride-based intracellular solutions (Bennett et al., 2019), in our study, Nav1.8 might constitute a majority of the TTX-R current.

PGE₂ (10 μM) robustly increased the current density of the TTX-S channel at 24 h posttreatment but had no measurable effect on the TTX-R current. A previous study reported that acute PGE₂ treatment increased TTX-S conductance but had no effect on its activation curve in some TTX-S-only DRG neurons (Tripathi et al., 2011). As TTX-S channels such as Nav1.3 and Nav1.7 can be activated by a low activation threshold (Bennett et al., 2019), the hyperpolarizing shift of the activation curve of total sodium current by 24-h PGE₂ treatment may be explained by the increase in TTX-S but not TTX-R current. The I–V curve was increased by 5-min and 24-h treatment of PGE₂ especially at approximately -5 mV and -25 mV, respectively, which could be explained by the increased TTX-R and TTX-S currents, respectively, for 5-min and 24-h treatment of PGE₂.

In our previous study, we found that 24-h treatment with PGE₂ in the TG ganglion increases the mRNA and protein levels of Nav1.7, underlying a mechanism in complete Freund's adjuvant (CFA)-induced TMJ inflammatory hyperalgesia (Zhang and Gan, 2017). In this study, 24-h treatment with PGE₂ (10 μM) increased the TTX-S current, which supports our previous work on Nav1.7 by showing a functional increase in the TTX-S current. We also observed that the mRNA of Nav1.1 was significantly increased by 24-h treatment with PGE₂, suggesting Nav1.1 probably also contribute to the increase of TTX-S current after prolonged treatment of PGE₂. Nav1.1 has been found expressed mainly in the medium-sized TG neurons, and it could be activated by subthreshold stimuli and contribute to mechanical hyperalgesia (Griffith et al., 2019; Osteen et al., 2016). TTX-S channels including Nav1.1 and Nav1.7 are crucial for the threshold and frequency of action potential in response to suprathreshold and subthreshold depolarization (Griffith et al., 2019; McDermott et al., 2019; Meents et al., 2019; Osteen et al., 2016), we hypothesized that 24-h treatment of PGE₂ may also contribute to the excitability of sensory neurons, which need to be investigated further in the future. The acute effect of PGE₂ on sodium current lasts less than 15 min (Gold et al., 1996); while the expression of mRNA and protein levels involved-prolonged effect of PGE₂ may contribute to a much longer time-course of the excitability (1–3 days for sodium channel turnover)

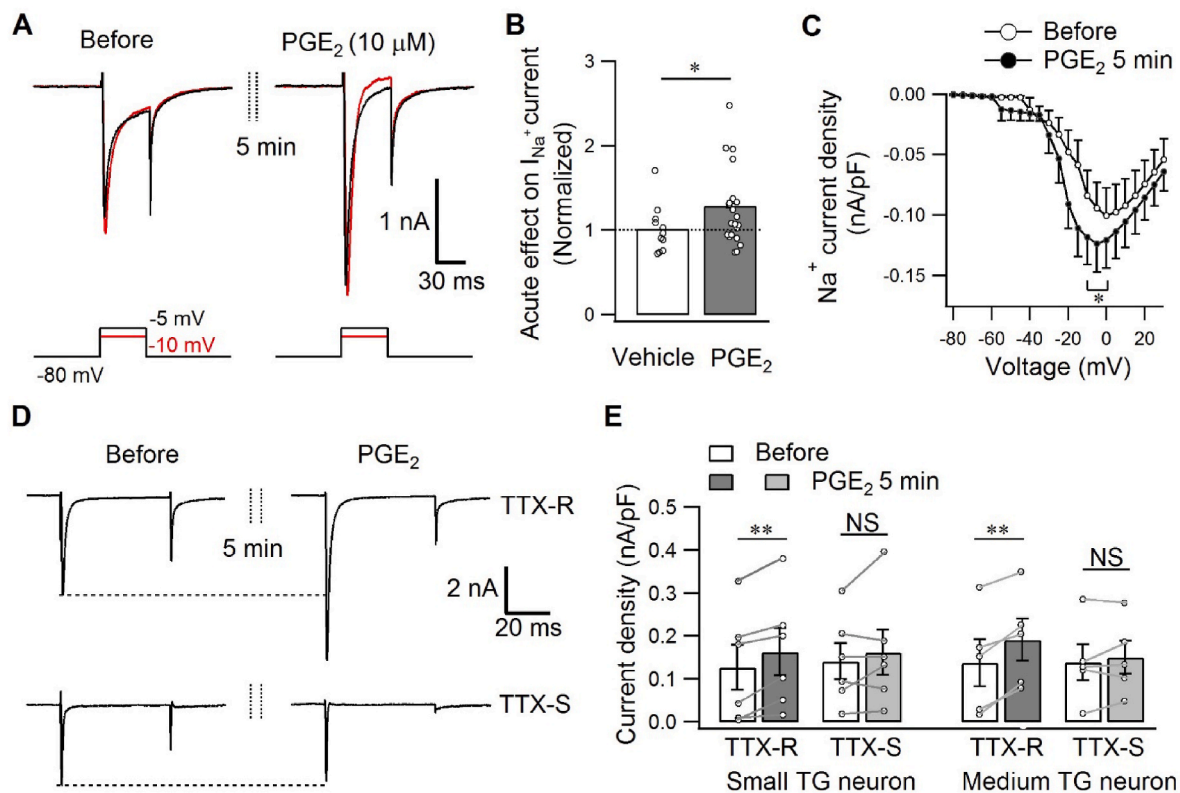


Fig. 5. Acute PGE₂ treatment increased TTX-R but not TTX-S currents in small- to medium-sized TG neurons. (A) Representative traces showing that the application of PGE₂ (10 μM) for 5 min increased the peak value of TG sodium currents when evoked from -80 mV to voltage steps of -10 mV (red) or -5 mV (black). (B) Normalized data showing the acute effect of PGE₂ on the peak value of sodium current density. (C) I-V curve of sodium current density in PGE₂-responsive neurons, with a significant change between -10 mV and 0 mV after the application of PGE₂. (D) Representative traces showing PGE₂ increased TTX-R but not TTX-S current after application for 5 min. (E) Statistics showing the acute effect of PGE₂ on the current densities of TTX-S and TTX-R channels in small- or medium-sized TG neurons. NS, no significance. Error bar, SEM. **P* < 0.05, ***P* < 0.01, Mann-Whitney test for (B), paired Student's *t*-test for (C) and (E).

(Devor, 2006; Porreca et al., 1999).

In the acute phase, 5-min PGE₂ (10 μM) treatment primarily increased the TTX-R current in TG neurons, but 24-h PGE₂ (10 μM) treatment predominantly increased TTX-S current. PGE₂ is acutely released several minutes or hours after surgery, simultaneously with pain onset (Buvanendran et al., 2006; Dionne et al., 2003; Roszkowski et al., 1997), and is maintained at a high level in persistent pain for months (Dirig and Yaksh, 1999; Guay et al., 2004; Hedo et al., 1999; Lin et al., 2015). A single injection of PGE₂ into the paw increases mechanical sensitivity within several minutes and lasts for 4–24 h (Huang et al., 2015; Kassuya et al., 2007; Ulmann et al., 2010), and daily injection of PGE₂ for two weeks induces chronic pain that lasts for months (Ferreira et al., 1990). Kinases are differentially involved during the initiation and chronification of pain syndrome; cAMP is involved in the onset of single PGE₂-induced paw mechanical hyperalgesia, while a PKA inhibitor is important both for the onset and maintenance of mechanical hyperalgesia, which lasts for approximately 3 h (Aley and Levine, 1999). PKA is required for hyperalgesia from 0 to 4 h during carrageenan-induced inflammation, but PKC is required 4 h post-inflammation (Huang et al., 2015). Therefore, we hypothesized that the sodium channel shift from TTX-R and TTX-S examined at 5 min and 24 h posttreatment with PGE₂ may be a cellular marker underlying the transition of PGE₂-mediated initiation and maintenance of inflammatory pain.

Proinflammatory mediators, such as PGE₂, IL-1β and TNF-α, have been widely studied on sodium currents after acute treatment of sensory neurons (Binshtok et al., 2008; Jin and Gereau, 2006), while the different functions of PGE₂ on subtypes of sodium channels between acute and prolonged treatments suggest that the acute and prolonged effects may not be regarded simply as the same.

The TTX-S current was potentially increased at 24 h posttreatment with PGE₂ (10 μM) in medium-sized TG neurons, while acute treatment with PGE₂ (10 μM) increased the TTX-R current in both small- and medium-sized neurons. According to the classification of DRG/TG neuron types (Katagiri et al., 2012; Nakamura et al., 2016), small- and medium-sized TG neurons might include mostly C-type neurons and Aδ-type neurons, respectively. C- and Aδ-type afferent fibres are both involved in thermal and mechanical nociception. C-type fibres are mostly responsible for warm sensations and burning or dull pain, while Aδ fibres are responsible for pinprick pain and cold sensations (Beissner et al., 2010; Haggard et al., 2013). Therefore, PGE₂ may influence the quality of pain sensation during exposure for various durations by modulating subtypes of sodium currents in different afferent neurons. Following our previous work (Zhang and Gan, 2017), and to reduce the unnecessary distraction included by effect of estrogen on sodium channels in female rats (Hu et al., 2012; Wang et al., 2013), we only used male rats in the present study. But the results got in male animals may not be simply regarded as the same as in female, so future studies of both sexes are very important.

In conclusion, we observed that acute PGE₂ (10 μM) application increased TTX-R but not TTX-S current in both small- and medium-sized neurons. Prolonged PGE₂ (10 μM) increased TG sodium currents through a potent increase in current densities in TTX-S but not the TTX-R subtype in medium- but not small-sized TG neurons. This result suggests an important shift of TTX-R and TTX-S channels in PGE₂-mediated hyperalgesia during the development of orofacial persistent pain.

5. Conclusions

Taken together, we found that acute and prolonged PGE₂ treatment increased the amplitude of sodium current and augmented the peak

value of sodium current density in small-to medium-sized TG neurons. Prolonged PGE₂ treatment shifted the activation curve in the hyperpolarizing direction and increased the peak value of TTX-S but not the TTX-R current density in medium- but not small-sized TG neurons. Acute PGE₂ increased TTX-R but not TTX-S current in both small- and medium-sized TG neurons, suggesting a different role of TTX-S and TTX-R currents in PGE₂-mediated acute and persistent nociceptive signalling, which is potentially useful for understanding the mechanisms underlying the development of orofacial persistent pain.

Funding

This work was sponsored by National Natural Science Foundation of China (31600950) and Clinical Medicine Plus X-Young Scholars Project, Peking University, the Fundamental Research Funds for the Central Universities (PKU2022LCXQ024).

Date availability statement

Data is contained within the article.

CRedit authorship contribution statement

Xiao-Yu Zhang: Data curation, Formal analysis, Writing – original draft, Writing – review & editing, performed the experiments, participated in data analysis and wrote the paper. **Xi Wu:** Data curation, Formal analysis, Writing – review & editing, Writing – original draft, performed the experiments, participated in data analysis. **Peng Zhang:** Data curation, Formal analysis, Writing – review & editing, Writing – original draft, participated in data analysis, performed the experiments. **Ye-Hua Gan:** Writing – original draft, Writing – review & editing, designed this research and wrote the paper. All authors contributed substantially to this research and reviewed this manuscript.

Declaration of competing interest

The authors declare no conflict of interest.

Acknowledgements

We thank Renee Cockerham for language help and Yanqiao Wang for data analysis support.

Appendix A. Supplementary data

Supplementary data to this article can be found online at <https://doi.org/10.1016/j.neuropharm.2022.109156>.

References

- Aley, K.O., Levine, J.D., 1999. Role of protein kinase A in the maintenance of inflammatory pain. *J. Neurosci.* 19, 2181–2186.
- Basbaum, A.I., Bautista, D.M., Scherrer, G., Julius, D., 2009. Cellular and molecular mechanisms of pain. *Cell* 139, 267–284.
- Beissner, F., Brandau, A., Henke, C., Felden, L., Baumgartner, U., Treede, R.D., Oertel, B. G., Lotsch, J., 2010. Quick discrimination of A(delta) and C fiber mediated pain based on three verbal descriptors. *PLoS One* 5, e12944.
- Bennett, D.L., Clark, A.J., Huang, J., Waxman, S.G., Dib-Hajj, S.D., 2019. The role of voltage-gated sodium channels in pain signaling. *Physiol. Rev.* 99, 1079–1151.
- Binshtok, A.M., Wang, H., Zimmermann, K., Amaya, F., Vardeh, D., Shi, L., Brenner, G.J., Ji, R.R., Bean, B.P., Woolf, C.J., Samad, T.A., 2008. Nociceptors are interleukin-1beta sensors. *J. Neurosci.* 28, 14062–14073.
- Black, J.A., Liu, S., Tanaka, M., Cummins, T.R., Waxman, S.G., 2004a. Changes in the expression of tetrodotoxin-sensitive sodium channels within dorsal root ganglia neurons in inflammatory pain. *Pain* 108, 237–247.
- Black, J.A., Liu, S., Tanaka, M., Cummins, T.R., Waxman, S.G., 2004b. Changes in the expression of tetrodotoxin-sensitive sodium channels within dorsal root ganglia neurons in inflammatory pain. *Pain* 108, 237–247.
- Buvanendran, A., Kroin, J.S., Berger, R.A., Hallab, N.J., Saha, C., Negrescu, C., Moric, M., Caicedo, M.S., Tuman, K.J., 2006. Upregulation of prostaglandin E2 and interleukins in the central nervous system and peripheral tissue during and after surgery in humans. *Anesthesiology* 104, 403–410.
- Cummins, T.R., Dib-Hajj, S.D., Black, J.A., Akopian, A.N., Wood, J.N., Waxman, S.G., 1999. A novel persistent tetrodotoxin-resistant sodium current in SNS-null and wild-type small primary sensory neurons. *J. Neurosci.* 19, RC43.
- Cummins, T.R., Waxman, S.G., 1997. Downregulation of tetrodotoxin-resistant sodium currents and upregulation of a rapidly repriming tetrodotoxin-sensitive sodium current in small spinal sensory neurons after nerve injury. *J. Neurosci.* 17, 3503–3514.
- Davidson, S., Golden, J.P., Copits, B.A., Ray, P.R., Vogt, S.K., Valtcheva, M.V., Schmidt, R.E., Ghetti, A., Price, T.J., Gereau, R.W.t., 2016. Group II mGluRs suppress hyperexcitability in mouse and human nociceptors. *Pain* 157, 2081–2088.
- Devor, M., 2006. Sodium channels and mechanisms of neuropathic pain. *J. Pain* 7, S3–S12.
- Dib-Hajj, S.D., Cummins, T.R., Black, J.A., Waxman, S.G., 2010. Sodium channels in normal and pathological pain. *Annu. Rev. Neurosci.* 33, 325–347.
- Dib-Hajj, S.D., Fjell, J., Cummins, T.R., Zheng, Z., Fried, K., LaMotte, R., Black, J.A., Waxman, S.G., 1999. Plasticity of sodium channel expression in DRG neurons in the chronic constriction injury model of neuropathic pain. *Pain* 83, 591–600.
- Dionne, R.A., Gordon, S.M., Rowan, J., Kent, A., Brahim, J.S., 2003. Dexamethasone suppresses peripheral prostanoid levels without analgesia in a clinical model of acute inflammation. *J. Oral Maxillofac. Surg.* 61, 997–1003.
- Dirig, D.M., Yaksh, T.L., 1999. In vitro prostanoid release from spinal cord following peripheral inflammation: effects of substance P, NMDA and capsaicin. *Br. J. Pharmacol.* 126, 1333–1340.
- Djouhri, L., Lawson, S.N., 2004. Abeta-fiber nociceptive primary afferent neurons: a review of incidence and properties in relation to other afferent A-fiber neurons in mammals. *Brain Res Brain Res Rev* 46, 131–145.
- England, S., Bevan, S., Docherty, R.J., 1996. PGE2 modulates the tetrodotoxin-resistant sodium current in neonatal rat dorsal root ganglion neurones via the cyclic AMP-protein kinase A cascade. *J. Physiol.* 495 (Pt 2), 429–440.
- Ferreira, S.H., Lorenzetti, B.B., De Campos, D.I., 1990. Induction, blockade and restoration of a persistent hypersensitive state. *Pain* 42, 365–371.
- Fitzgerald, E.M., Okuse, K., Wood, J.N., Dolphin, A.C., Moss, S.J., 1999. cAMP-dependent phosphorylation of the tetrodotoxin-resistant voltage-dependent sodium channel SNS. *J. Physiol.* 516 (Pt 2), 433–446.
- Gold, M.S., Levine, J.D., Correa, A.M., 1998. Modulation of TTX-R INa by PKC and PKA and their role in PGE2-induced sensitization of rat sensory neurons in vitro. *J. Neurosci.* 18, 10345–10355.
- Gold, M.S., Reichling, D.B., Shuster, M.J., Levine, J.D., 1996. Hyperalgesic agents increase a tetrodotoxin-resistant Na⁺ current in nociceptors. *Proc. Natl. Acad. Sci. U. S. A.* 93, 1108–1112.
- Gold, M.S., Traub, R.J., 2004. Cutaneous and colonic rat DRG neurons differ with respect to both baseline and PGE2-induced changes in passive and active electrophysiological properties. *J. Neurophysiol.* 91, 2524–2531.
- Griffith, T.N., Docter, T.A., Lumpkin, E.A., 2019. Tetrodotoxin-sensitive sodium channels mediate action potential firing and excitability in menthol-sensitive vglut3-lineage sensory neurons. *J. Neurosci.* 39, 7086–7101.
- Guay, J., Bateman, K., Gordon, R., Mancini, J., Riendeau, D., 2004. Carrageenan-induced paw edema in rat elicits a predominant prostaglandin E2 (PGE2) response in the central nervous system associated with the induction of microsomal PGE2 synthase-1. *J. Biol. Chem.* 279, 24866–24872.
- Haggard, P., Iannetti, G.D., Longo, M.R., 2013. Spatial sensory organization and body representation in pain perception. *Curr. Biol.* 23, R164–R176.
- Hedo, G., Laird, J.M., Lopez-Garcia, J.A., 1999. Time-course of spinal sensitization following carrageenan-induced inflammation in the young rat: a comparative electrophysiological and behavioural study in vitro and in vivo. *Neuroscience* 92, 309–318.
- Hu, F., Wang, Q., Wang, P., Wang, W., Qian, W., Xiao, H., Wang, L., 2012. 17beta-Estradiol regulates the gene expression of voltage-gated sodium channels: role of estrogen receptor alpha and estrogen receptor beta. *Endocrine* 41, 274–280.
- Huang, W.Y., Dai, S.P., Chang, Y.C., Sun, W.H., 2015. Acidosis mediates the switching of gs-PKA and gi-PKC dependence in prolonged hyperalgesia induced by inflammation. *PLoS One* 10, e0125022.
- Jin, X., Gereau, R.W.t., 2006. Acute p38-mediated modulation of tetrodotoxin-resistant sodium channels in mouse sensory neurons by tumor necrosis factor-alpha. *J. Neurosci.* 26, 246–255.
- Kadoi, J., Takeda, M., Matsumoto, S., 2007. Prostaglandin E2 potentiates the excitability of small diameter trigeminal root ganglion neurons projecting onto the superficial layer of the cervical dorsal horn in rats. *Exp. Brain Res.* 176, 227–236.
- Kassuya, C.A., Ferreira, J., Claudino, R.F., Calixto, J.B., 2007. Intraplantar PGE2 causes nociceptive behaviour and mechanical allodynia: the role of prostanoid E receptors and protein kinases. *Br. J. Pharmacol.* 150, 727–737.
- Katagiri, A., Shinoda, M., Honda, K., Toyofuku, A., Sessle, B.J., Iwata, K., 2012. Satellite glial cell P2Y12 receptor in the trigeminal ganglion is involved in lingual neuropathic pain mechanisms in rats. *Mol. Pain* 8, 23.
- Kral, M.G., Xiong, Z., Study, R.E., 1999. Alteration of Na⁺ currents in dorsal root ganglion neurons from rats with a painful neuropathy. *Pain* 81, 15–24.
- Lin, C.C., Hsieh, H.L., Liu, S.W., Tseng, H.C., Hsiao, L.D., Yang, C.M., 2015. BK induces cPLA2 expression via an autocrine loop involving COX-2-derived PGE2 in rat brain astrocytes. *Mol. Neurobiol.* 51, 1103–1115.
- Liu, H., Duan, S.R., 2016. Prostaglandin E2-mediated upregulation of neuroexcitation and persistent tetrodotoxin-resistant Na(+) currents in Ah-type trigeminal ganglion neurons isolated from adult female rats. *Neuroscience* 320, 194–204.
- Liu, L., Karagoz, H., Herneisey, M., Zor, F., Komatsu, T., Loftus, S., Janjic, B.M., Gorantla, V.S., Janjic, J.M., 2020. Sex differences revealed in a mouse CFA

- inflammation model with macrophage targeted nanotheranostics. *Theranostics* 10, 1694–1707.
- Liu, Y., Xu, X.X., Cao, Y., Mo, S.Y., Bai, S.S., Fan, Y.Y., Zhang, X.Y., Xie, Q.F., 2021. 17beta-Estradiol exacerbated experimental occlusal interference-induced chronic masseter hyperalgesia by increasing the neuronal excitability and TRPV1 function of trigeminal ganglion in ovariectomized rats. *Int. J. Mol. Sci.* 22.
- Lopes, D.M., Denk, F., McMahon, S.B., 2017. The molecular fingerprint of dorsal root and trigeminal ganglion neurons. *Front. Mol. Neurosci.* 10, 304.
- Ma, W., Chabot, J.G., Vercauteren, F., Quirion, R., 2010. Injured nerve-derived COX2/PGE2 contributes to the maintenance of neuropathic pain in aged rats. *Neurobiol. Aging* 31, 1227–1237.
- Ma, W., Eisenach, J.C., 2003. Cyclooxygenase 2 in infiltrating inflammatory cells in injured nerve is universally up-regulated following various types of peripheral nerve injury. *Neuroscience* 121, 691–704.
- Malty, R.H., Hudmon, A., Fehrenbacher, J.C., Vasko, M.R., 2016. Long-term exposure to PGE2 causes homologous desensitization of receptor-mediated activation of protein kinase A. *J. Neuroinflammation* 13, 181.
- McDermott, L.A., Weir, G.A., Themistocleous, A.C., Segerdahl, A.R., Blesneac, I., Baskozos, G., Clark, A.J., Millar, V., Peck, L.J., Ebner, D., Tracey, I., Serra, J., Bennett, D.L., 2019. Defining the functional role of Nav1.7 in human nociception. *Neuron* 101, 905–919 e908.
- Meents, J.E., Bressan, E., Sontag, S., Foerster, A., Hautvast, P., Rosseler, C., Hampl, M., Schuler, H., Goetzke, R., Le, T.K.C., Kleggetveit, I.P., Le Cann, K., Kerth, C., Rush, A. M., Rogers, M., Kohl, Z., Schmelz, M., Wagner, W., Jorum, E., Namer, B., Winner, B., Zenke, M., Lampert, A., 2019. The role of Nav1.7 in human nociceptors: insights from human induced pluripotent stem cell-derived sensory neurons of erythromelalgia patients. *Pain* 160, 1327–1341.
- Megat, S., Ray, P.R., Tavares-Ferreira, D., Moy, J.K., Sankaranarayanan, I., Wangzhou, A., Fang Lou, T., Barragan-Iglesias, P., Campbell, Z.T., Dussor, G., Price, T.J., 2019. Differences between dorsal root and trigeminal ganglion nociceptors in mice revealed by translational profiling. *J. Neurosci.* 39, 6829–6847.
- Nakamura, M., Kim, D.Y., Jang, I.S., 2016. Acid modulation of tetrodotoxin-sensitive Na(+) channels in large-sized trigeminal ganglion neurons. *Brain Res.* 1651, 44–52.
- Osteen, J.D., Herzig, V., Gilchrist, J., Emrick, J.J., Zhang, C., Wang, X., Castro, J., Garcia-Caraballo, S., Grundy, L., Rychkov, G.Y., Weyer, A.D., Dekan, Z., Undheim, E.A., Alewood, P., Stucky, C.L., Briery, S.M., Basbaum, A.I., Bosmans, F., King, G.F., Julius, D., 2016. Selective spider toxins reveal a role for the Nav1.1 channel in mechanical pain. *Nature* 534, 494–499.
- Petho, G., Reeh, P.W., 2012. Sensory and signaling mechanisms of bradykinin, eicosanoids, platelet-activating factor, and nitric oxide in peripheral nociceptors. *Physiol. Rev.* 92, 1699–1775.
- Porreca, F., Lai, J., Bian, D., Wegert, S., Ossipov, M.H., Eglén, R.M., Kassotakis, L., Novakovic, S., Rabert, D.K., Sangameswaran, L., Hunter, J.C., 1999. A comparison of the potential role of the tetrodotoxin-insensitive sodium channels, PN3/SNS and NaN/SNS2, in rat models of chronic pain. *Proc. Natl. Acad. Sci. U. S. A.* 96, 7640–7644.
- Roszkowski, M.T., Swift, J.Q., Hargreaves, K.M., 1997. Effect of NSAID administration on tissue levels of immunoreactive prostaglandin E2, leukotriene B4, and (S)-flurbiprofen following extraction of impacted third molars. *Pain* 73, 339–345.
- Samad, T.A., Saperstein, A., Woolf, C.J., 2002. Prostanoids and pain: unraveling mechanisms and revealing therapeutic targets. *Trends Mol. Med.* 8, 390–396.
- Tanaka, M., Cummins, T.R., Ishikawa, K., Dib-Hajj, S.D., Black, J.A., Waxman, S.G., 1998. SNS Na+ channel expression increases in dorsal root ganglion neurons in the carrageenan inflammatory pain model. *Neuroreport* 9, 967–972.
- Tate, S., Benn, S., Hick, C., Trezise, D., John, V., Mannion, R.J., Costigan, M., Plumpton, C., Grose, D., Gladwell, Z., Kendall, G., Dale, K., Bountra, C., Woolf, C.J., 1998. Two sodium channels contribute to the TTX-R sodium current in primary sensory neurons. *Nat. Neurosci.* 1, 653–655.
- Treutlein, E.M., Kern, K., Weigert, A., Tarighi, N., Schuh, C.D., Nusing, R.M., Schreiber, Y., Ferreiros, N., Brune, B., Geisslinger, G., Pierre, S., Scholich, K., 2018. The prostaglandin E2 receptor EP3 controls CC-chemokine ligand 2-mediated neuropathic pain induced by mechanical nerve damage. *J. Biol. Chem.* 293, 9685–9695.
- Tripathi, P.K., Cardenas, C.G., Cardenas, C.A., Scroggs, R.S., 2011. Up-regulation of tetrodotoxin-sensitive sodium currents by prostaglandin E(2) in type-4 rat dorsal root ganglion cells. *Neuroscience* 185, 14–26.
- Ulmann, L., Hirbec, H., Rassendren, F., 2010. P2X4 receptors mediate PGE2 release by tissue-resident macrophages and initiate inflammatory pain. *EMBO J.* 29, 2290–2300.
- Vaughn, A.H., Gold, M.S., 2010. Ionic mechanisms underlying inflammatory mediator-induced sensitization of dural afferents. *J. Neurosci.* 30, 7878–7888.
- Wang, Q., Cao, J., Hu, F., Lu, R., Wang, J., Ding, H., Gao, R., Xiao, H., 2013. Effects of estradiol on voltage-gated sodium channels in mouse dorsal root ganglion neurons. *Brain Res.* 1512, 1–8.
- Watzer, B., Zehbe, R., Halstenberg, S., James Kirkpatrick, C., Brochhausen, C., 2009. Stability of prostaglandin E(2) (PGE (2)) embedded in poly-D,L-lactide-co-glycolide microspheres: a pre-conditioning approach for tissue engineering applications. *J. Mater. Sci. Mater. Med.* 20, 1357–1365.
- Xu, S., Ono, K., Inenaga, K., 2010. Electrophysiological and chemical properties in subclassified acutely dissociated cells of rat trigeminal ganglion by current signatures. *J. Neurophysiol.* 104, 3451–3461.
- Zhang, P., Bi, R.Y., Gan, Y.H., 2018a. Glial interleukin-1beta upregulates neuronal sodium channel 1.7 in trigeminal ganglion contributing to temporomandibular joint inflammatory hypernociception in rats. *J. Neuroinflammation* 15, 117.
- Zhang, P., Gan, Y.H., 2017. Prostaglandin E2 upregulated trigeminal ganglionic sodium channel 1.7 involving temporomandibular joint inflammatory pain in rats. *Inflammation* 40, 1102–1109.
- Zhang, X.Y., Bi, R.Y., Zhang, P., Gan, Y.H., 2018b. Veratridine modifies the gating of human voltage-gated sodium channel Nav1.7. *Acta Pharmacol. Sin.* 39, 1716–1724.